ChemistryEurope
Excellence in Chemistry Research Worldwide

Research Article
doi.org/10.1002/ceur.202500069

www.journal.chemistry-europe.org

# Self-Assembly of Silver Nanoclusters by Cooperative Acetylene Bonding with Mutual Pyridyl Coordination

Tasuki Tsurumi, Takahiro Nakagawa, Takashi Kikuchi, Kiyohiro Adachi, Hironobu Hayashi, Atsuro Takai, Takuma Kaneko, Tomoya Uruga, Daisuke Hashizume, Yosuke Nakamura, Makoto Fujita, and Yuya Domoto*

The controlled supramolecular alignment of atomically precise metal nanoclusters is a promising method to unlock unprecedented properties and advanced functions beyond those of the individual monomeric nanoclusters. Conventional protocols for the construction of such assemblies require the use of two or more types of ligands for protecting and interconnecting the nanoclusters, respectively. Herein, a strategy is demonstrated for the hierarchical self-assembly of an alkyne-protected silver nanocluster into a 3D network in the crystalline lattice based on cooperative silver···acetylene coordination and silver···pyridyl coordination by a bifunctional ligand with a simple design. The bent ligand **L** produces a $Cl@Ag_{14}L_{12}$ monomer with a helical conformation resembling that of organic tripodal ligands, which assembles into a 3D network as evident from a single-crystal X-ray diffraction analysis. The monomeric and network structures are further characterized using grazing-incidence small-angle X-ray scattering, atomic force microscopy, X-ray photoelectron spectroscopy, and X-ray absorption fine structure, in addition to photoluminescence with a microsecond lifetime in the solid state, exhibiting the success of the strategy toward the design of self-assembled 3D supramolecular arrangements of atomically precise metal nanoclusters using a single, simple ligand.

## 1. Introduction

Atomically precise coinage-metal nanoclusters (NCs) have emerged as unique molecular materials whose properties and functions can be tuned by the number of metals and their 3D geometry, as well as the installation of protectants and functional groups.[1–3] In addition, the spatial alignment of NCs to enhance their properties or obtain unprecedented functions has become a hot topic within the past decade. The connection of the NCs is usually achieved via noncovalent interactions, such as electrostatic interactions, hydrogen bonds, π–π stacking, and alkyl packing.[4,5] Additionally, the use of appropriate templates can also induce the regular assembly of NCs into hierarchical superstructures.[6]

In this context, metal coordination, particularly with nitrogen-containing heterocyclic donors, is a relatively new approach[7] despite its numerous applications in the field of coordination nanomaterials.[8,9] Pradeep and co-workers have reported the synthesis of an $Ag_{25}$ dimer by utilizing a thiolate ligand equipped with a bipyridyl moiety to form a Ru(II) complex as a junction.[7b] Tsukuda and co-workers have designed an $Au_{13}$ coaxially substituted with two alkynyl ligands bearing a terpyridyl group at

*T. Tsurumi, Y. Nakamura, Y. Domoto*
*Division of Molecular Science*
*Graduate School of Science and Technology*
*Gunma University*
*1-5-1 Tenjin-cho, Kiryu-shi, Gunma 376-8515, Japan*
*E-mail: domoto@gunma-u.ac.jp*

*T. Nakagawa, M. Fujita*
*Tokyo College*
*U-Tokyo Institutes for Advanced Study (UTIAS)*
*The University of Tokyo, Mitsui Link Lab Kashiwanoha 1*
*FS CREATION*
*6-6-2 Kashiwanoha, Kashiwa-shi, Chiba 277-0882, Japan*

*T. Kikuchi*
*Rigaku Corporation*
*3-9-12 Matsubara-cho, Akishima-shi, Tokyo 196-8666, Japan*

*K. Adachi, D. Hashizume*
*RIKEN Center for Emergent Matter Science (CEMS)*
*Wako-shi, Saitama 351-0198, Japan*

*H. Hayashi*
*Center for Basic Research on Materials*
*National Institute for Materials Science (NIMS)*
*1-2-1 Sengen, Tsukuba-shi, Ibaraki 305-0047, Japan*

*A. Takai*
*Molecular Design and Function Group*
*National Institute for Materials Science (NIMS)*
*1-2-1 Sengen, Tsukuba-shi, Ibaraki 305-0047, Japan*

*T. Kaneko, T. Uruga*
*Japan Synchrotron Radiation Research Institute (JASRI/SPring-8)*
*Kouto, Sayo, Hyogo 679-5198, Japan*

*T. Uruga*
*Innovation Research Center for Fuel Cells*
*The University of Electro-Communications*
*Chofu, Tokyo 182-8585, Japan*

*M. Fujita*
*Division of Advanced Molecular Science*
*Institute for Molecular Science*
*National Institutes of Natural Sciences*
*5-1 Higashiyama, Myodaiji-cho, Okazaki-shi, Aichi 444-8787, Japan*

*Supporting information for this article is available on the WWW under https://doi.org/10.1002/ceur.202500069*

Research Article
doi.org/10.1002/ceur.202500069



each end, which forms linear complexes with 3*d* metal ions.[7c] NC-based metal–organic frameworks have also recently been exploited to prepare 3D arrangements.[10] In these cases, the protected NCs are bridged by additional bidentate pyridyl ligands; this approach thus requires both a protecting ligand and a ligand linkage (**Figure 1**a). Alternatively, direct extension via the self-assembly of coordination polymers[11,12] (Figure 1b) is a potentially promising approach for the facile construction of networked NCs. Here, we demonstrate the hierarchical assembly of silver NCs using a hetero-bidentate ligand with a pyridyl group at one end and a terminal alkyne moiety at the other (Figure 1d).

In addition to its use in the capping of NCs,[13,14] metal–acetylene coordination is ubiquitous in organometallic

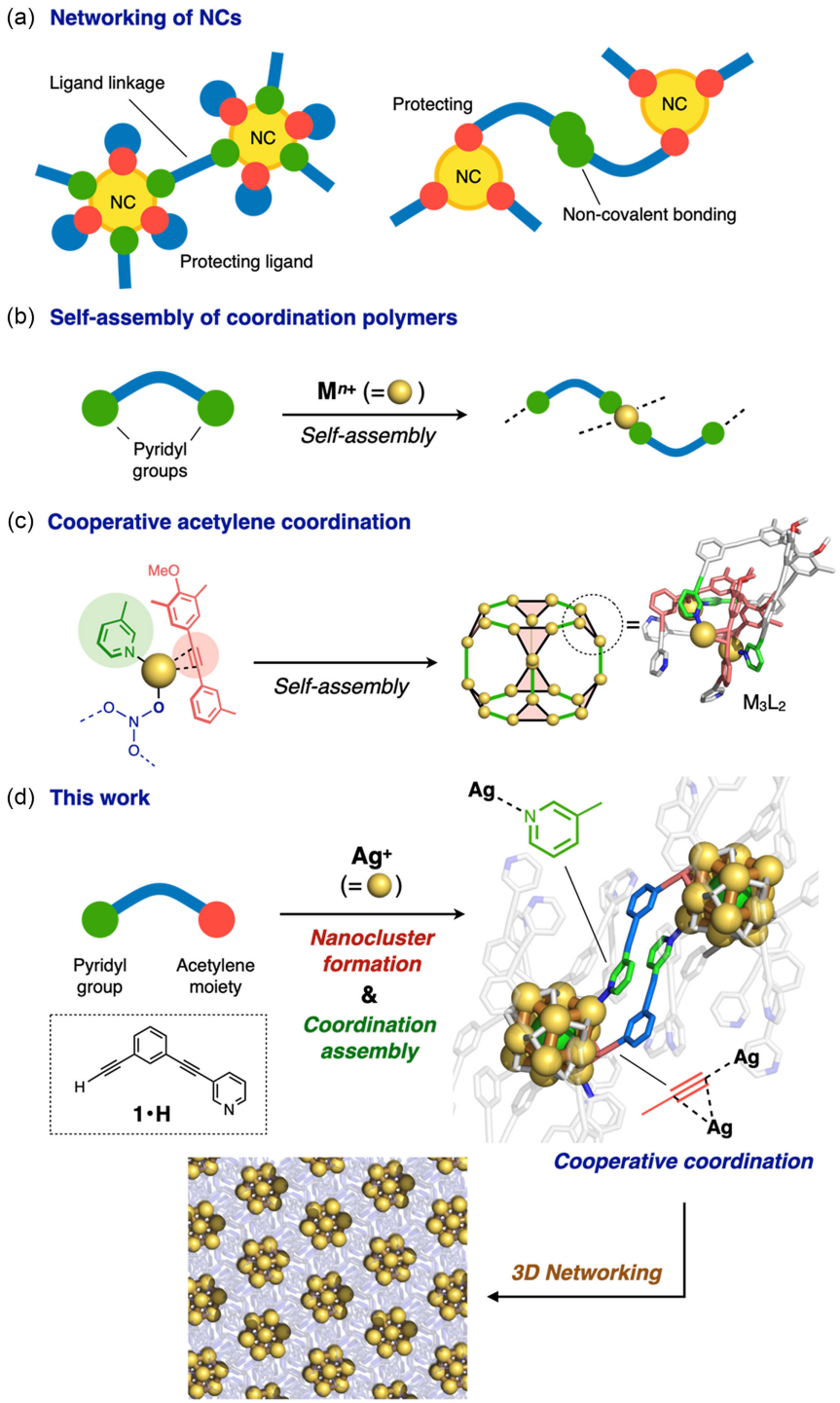


**Figure 1.** a) Conventional methods of interconnecting NCs based on separate protective capping and networking steps. b) Self-assembly of coordination polymers. c) Cooperative acetylene coordination to give polyhedral cages composed of $M_3L_2$-type subunits.[18c] d) Schematic representation of the self-assembly of NCs via a ligand realizing cooperative coordination. The chemical structure of ligand **1•H** is also shown.

Research Article
doi.org/10.1002/ceur.202500069



chemistry,[15] and these relatively weak and loosely directed interactions have also been applied to host–guest systems,[16] structurally regulated foldamers,[17a] and other exotic nanoarchitectures.[17b,c] We have recently developed an approach of self-assembly based on cooperative acetylene coordination, i.e., acetylene π-coordination working in concert with coordination by a pyridyl and/or oxygen donor at the same metal center (Cu(I) or Ag(I)) (Figure 1c).[18,19] Acetylene coordination was revealed to be sufficiently flexible to realize the formation of a class of large (up to 5 nm) polyhedral cages with highly entangled structures[18a,c] that exhibit unique properties such as cocrystallization in infinitely networked lattices,[18b] precisely controlled topological chirality,[18d] and sequential interconversion upon anion exchange.[18c,e,f] These findings inspired us to apply this method to the construction of alkyne-protected NCs functionalized with pyridine coordinating groups, which can serve as monomer units for 3D assemblies of NCs.

## 2. Results and Discussion

First, the simple bifunctional ligand **1•H**, which has a terminal acetylene moiety at one end and a 3-pyridyl group at the other, was designed and prepared in a moderate total yield (for details, see the Supporting Information). A curved skeleton composed of a 1,3-disubstituted benzene ring and a 3-pyridyl moiety was chosen rather than a linear motif, as we expected that this would result in the generation of complexes with good single-crystal molecular packing like that observed in our previous self-assembly studies using tripodal ligands.[18] In fact, complexation of the 4-pyridyl analogue with silver trifluoromethane sulfonate (AgOTf) using the conditions described below failed to provide any crystals. The ligand can also be fine-tuned, for example, by introducing a small functional group (dimethylamino group in the case of **2•H**) in the central benzene ring (Figure S1, Supporting Information).

When ligand **1•H** was treated with AgOTf (1.0 eq., 5.0 mM) in dichloromethane/$Et_3N$ (9:1), the initial generation of a silver acetylide was confirmed by $^1H$ NMR spectroscopy, which showed the diminished signal for the terminal alkyne proton (Figure S2, Supporting Information). A cloudy precipitate formed immediately upon complexation, and after incubation for 6 days at 5 °C, slightly yellowish single crystals were obtained (Figure S3, Supporting Information). Scanning electron microscopy measurements revealed rhombohedral crystals with diameters of 10–20 μm (Figure S4, Supporting Information). Notably, crystal formation was not observed when the precipitate was filtered out, indicating that the kinetic formation of the precipitate is essential to nuclei formation under the applied conditions.

An X-ray diffraction analysis revealed the formation of the complex $Cl@Ag_{14}(\mathbf{1})_{12}$, which crystallizes in the trigonal space group *R*-3 (**Figure 2**a and Table S1, Supporting Information).[20] The core structure is composed of two layers of silver atoms forming an $Ag_6$ octagon (A) and an $Ag_8$ cube (B), respectively, and the structure encapsulates a chloride ion in its central cavity (Figure 2b, S5 and S6, Supporting Information). The Ag···Ag distances between layers A and B are 2.91–3.10 Å, which is

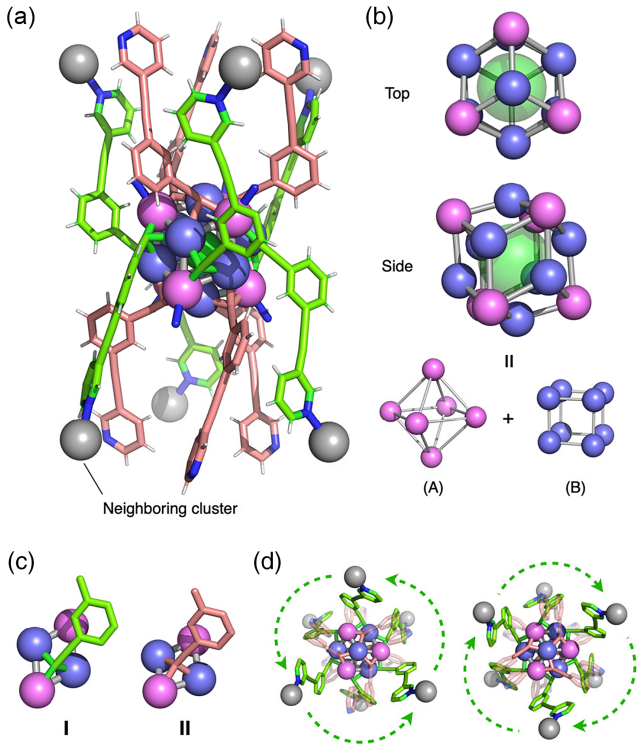


**Figure 2.** Single-crystal X-ray diffraction structure of the interconnected $Cl@Ag_{14}(\mathbf{1})_{12}$ NC (OTf salt). a) Monomeric structure; ligands coordinating to the neighboring clusters are shown in green, while free ligands are depicted in pale red. Blue sticks on the Ag atom indicate coordination by pyridyl groups of neighboring monomers. b) Detailed structure of the $Cl@Ag_{14}$ core. c) Coordination modes of the silver···acetylene capping. d) Helical configuration of the coordinating ligands as seen from the top and bottom of the monomer, respectively.

consistent with those observed in a discrete $Cl@Ag_{14}(C{\equiv}C\mathit{t}Bu)_{12}$ cluster previously reported by Mingos and co-workers.[21a] This result indicates that the ligand arms of **1** do not perturb the core structure. This type of chloride-templated NC formation has led to further enlargement[22] and shape modification of NCs.[23] The source of chloride in this study is unclear; however, examples of the formation of discrete Cl-encapsulating Ag NCs via extraction of Cl from dichloromethane have been reported.[24] Attempts at crystallization in other solvents, such as toluene, failed in our case. Additionally, active use of tetrabutylammonium chloride or NaCl was unsuccessful, possibly because the counter cation prevented the smooth single-crystal growth. Therefore, it is assumed that in situ generation of the chloride ion is crucial to obtain the networked structure. The coordination self-assembly enabled the networked $Cl@Ag_{14}$ clusters to be formed via simple mixing of the metal ion and the organic bifunctional ligand, unlike the discrete analogue, which often requires preparation from an explosive precursor containing aggregated silver acetylide.[21b]

In terms of the acetylene capping, two slightly different coordination environments were observed in the asymmetric unit (Figure 2c). Site I involves σ-coordination (Ag···C distance: 2.12 Å) and two π-coordination interactions (Ag···C: 2.33–2.78 Å), while site II exhibits three σ-coordination bonds (Ag···C: 2.17–2.35 Å). A terminal 3-pyridyl group of the ligand at site I

Research Article
doi.org/10.1002/ceur.202500069



coordinates to a silver atom in the neighboring cluster, while that of the ligand at site II exists as a free pyridyl group in the packing.

In addition to the coordination modes on the surface of the $Ag_{14}$ rhombic dodecahedral core described above, the bent shape of ligand **1** contributes to the helical tripodal configuration of the terminal 3-pyridyl groups attached to the $Ag_{14}$ core (Figure 2d), which resembles those of organic tripodal ligands that have been adopted in the self-assembly of the topological architectures.[19] The monomeric $Cl@Ag_{14}L_{12}$ would be not optically active because the helical shapes of the upper and lower tripodal arms cancel each other, as observed in the crystal structure. This conformation resulted in the formation of an infinite lattice characterized by mutual coordination affording the alignment of the $Ag_{14}$ cores with an intercluster distance of 1.7 nm (**Figure 3**a). Six silver atoms of each $Ag_{14}$ monomer core are coordinated by six ligands; each of these six ligands coordinates to a different neighboring monomer (Figure 2a and 3b). Along the *c*-axis, the $Cl@Ag_{14}$ clusters are in different positions in each of the three layers, forming a rhombic corner in each layer (Figure 3c,d). The contribution from π–π stacking (π···π: 2.9–3.5 Å) between the three types of ligands shown in Figure 3a is expected to be a stabilizing factor of the 3D network in the crystalline state. Consequently, this structure was preserved when the counter anion was changed to $SbF_6^-$, i.e., the crystals obtained when the synthesis was repeated using $AgSbF_6$ rather than AgOTf exhibited the same packing diagram (Figure S7, S8 and Table S1, Supporting Information).

The uniformity of the NCs formed in dichloromethane was confirmed via a grazing-incidence small-angle X-ray scattering (SAXS) analysis of the evaporated powder sample on a mica surface (Figure S9 and S10, Supporting Information). Three peaks were observed at $2\theta = 5.9°$, 6.7°, and 7.0° in the SAXS region, which are roughly consistent with those that were simulated based on the single-crystal structure. In contrast, no sharp signal was observed for the sample obtained by mixing **1**•**H** and AgOTf in nitromethane in the presence of triethylamine, which lacked specific molecular order upon evaporation.

Additionally, we used atomic-force microscopy (AFM) to examine the dispersibility of the monomeric $Cl@Ag_{14}(\mathbf{1})_{12}$ species outside the 3D networked lattice. Initial AFM image showed severely aggregated forms on the mica surface, while spin-coated samples treated with chloroform revealed relatively well-dispersed objects with a height of ≈1.6–1.8 nm (**Figure 4**a, S11, and S12, Supporting Information), which is consistent with the estimated size of monomeric $Cl@Ag_{14}(\mathbf{1})_{12}$, implying its stability. In contrast, all our attempts to observe the monomeric species by electrospray-ionization mass spectroscopy resulted in the detection of many fragmental peaks, including several assignable multiply charged ions (Figure S13, Supporting Information), possibly due to the lability of the $Ag_{14}$ core under the applied

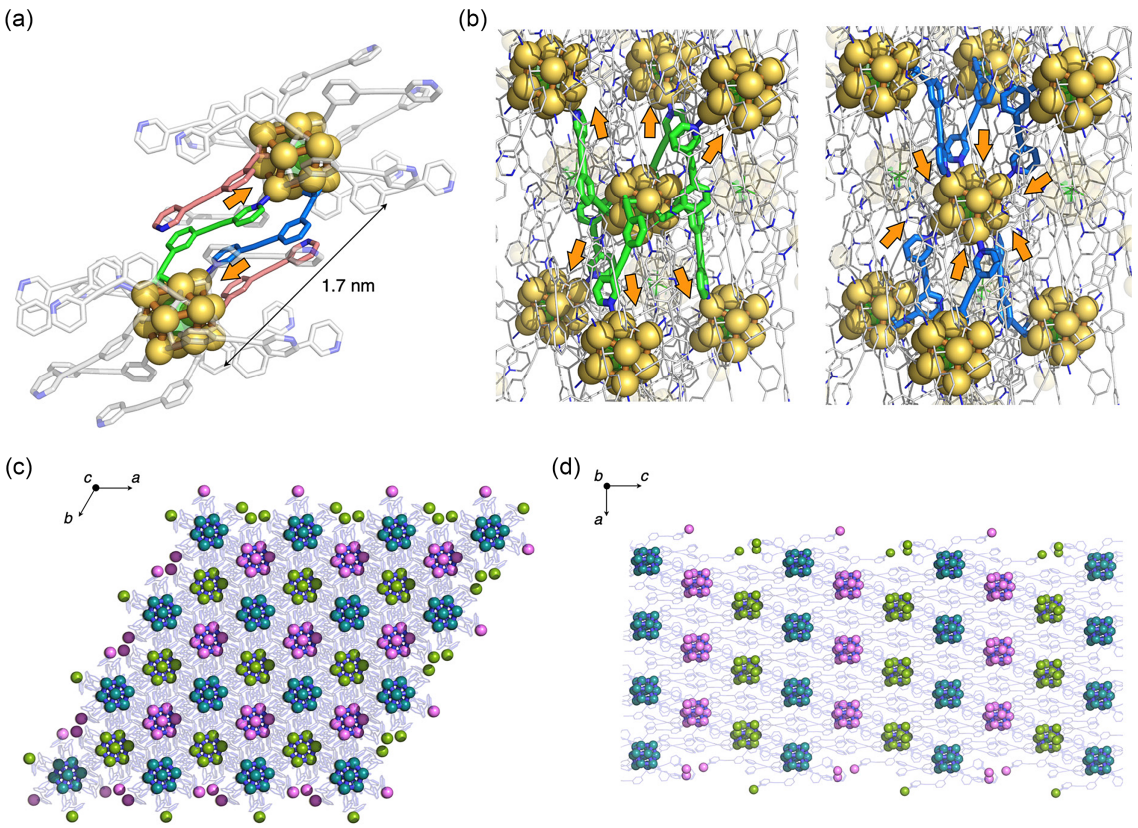


**Figure 3.** Interconnected structure of $Cl@Ag_{14}(\mathbf{1})_{12}$. a) Mutual coordination of the neighboring monomers via pyridyl groups. Focusing on the left monomer, the coordinating ligands are depicted in green, while the coordinated ones derived from the adjacent monomer are shown in blue. Ligands with free pyridyl groups are depicted in pale red. b) Schematic representation of the packing structure. Focusing on the central monomer, the coordinating ligands are depicted in green, while the coordinated ones derived from adjacent monomers are shown in blue. c) Packing structure along the *c*-axis. The $Cl@Ag_{14}$ cores in each of the three layers are depicted in blue, pink, and green, respectively. d) Packing structure along the *b*-axis.

Research Article
doi.org/10.1002/ceur.202500069



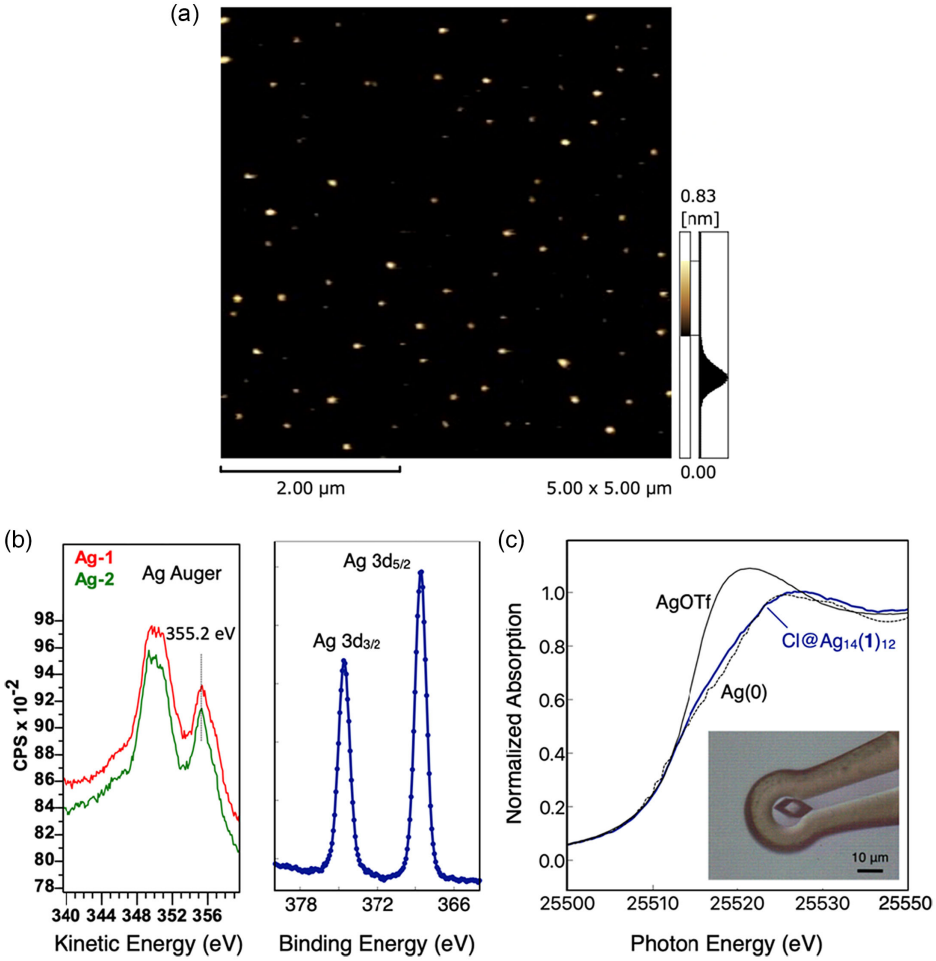


**Figure 4.** a) AFM image of Cl@$Ag_{14}$(**1**)$_{12}$ on a mica substrate. A detailed size distribution is shown in Figure S12 and S13, Supporting Information. b) XPS spectra of Cl@$Ag_{14}$(**1**)$_{12}$ in the Ag Auger region (left) and Ag 3*d* region (right). For the Auger region, measurements at two different positions on the sample (Ag-1 and Ag-2; Figure S14, Supporting Information) are shown. c) XANES spectrum of a single crystal of Cl@$Ag_{14}$(**1**)$_{12}$. For comparison, the spectra of AgOTf (black solid line) and Ag foil (black dotted line) are also shown. The inset represents a photograph of the measured single crystal mounted on the loop.

ionizing conditions in the absence of intercluster pyridyl coordination.

To elucidate the electronic states of the Cl@$Ag_{14}$ cluster, X-ray photoelectron spectroscopy (XPS) was conducted on a powdered sample (Figure 4b and S14, Supporting Information). In the Ag 3*d* region,[25,26a] two peaks were observed at 374.6 eV (Ag 3$d_{3/2}$) and 368.5 eV (Ag 3$d_{5/2}$) and an Auger peak appeared at 355.2 eV. Considering that the calculated Auger parameter of 723.7 eV is identical to that of $AgNO_3$ (723.8 eV) and significantly lower than that of $Ag^0$ (726.5 eV),[26b] we concluded that the silver centers presumably adopt predominantly the $Ag^I$ state. Curve-fitting analysis for the Ag 3*d* peaks mentioned above also supported this result, although the peaks for Ag(I) and Ag(0) are in close proximity to each other to be exactly determined. X-ray absorption spectroscopy measurements in the single-crystalline state were also performed using the quick X-ray absorption fine strcuture method[27,28] to avoid severe irradiation damage to the crystals, while the analysis with a shorter irradiation time gave almost identical results (Figure S15, Supporting Information). The Ag K-edge X-ray absorption near edge structure (XANES) spectrum of Cl@$Ag_{14}$(**1**)$_{12}$ indicated that the coordination environments of the NC have a relatively similar character to that of the metal Ag (Figure 4c), indicating the partial presence of Ag(0) depending on conditions.[25]

A solid fabricated by evaporating a solution of Cl@$Ag_{14}$(**1**)$_{12}$ exhibited orange emission upon photoexcitation (**Figure 5**a, inset). The UV–vis absorption spectrum of the solid is consistent with that of the crystals (Figure S16, Supporting Information). Photoluminescence spectroscopy in the solid state at 163 K exhibited an emission peak at 570 nm upon excitation at 470 nm, and variable-temperature measurements revealed an increase of emission intensity as the temperature was decreased from 303 to 163 K (Figure 5a and S18, Supporting Information).[29,30] This tendency is reasonable, considering that the Ag···Ag interactions in the cluster are dynamically affected by temperature change.[3b,31,32] The emission property was further studied by lifetime measurements at 173 K, which showed decay lifetimes of 1.8 µs and 4.8 ns ($\lambda_{em}$ = 560 nm; Figure 5b). Given that the silver centers of Cl@$Ag_{14}$(**1**)$_{12}$ are primarily in the Ag(I) state, which should be a closed shell system, the existence of the

Research Article
doi.org/10.1002/ceur.202500069



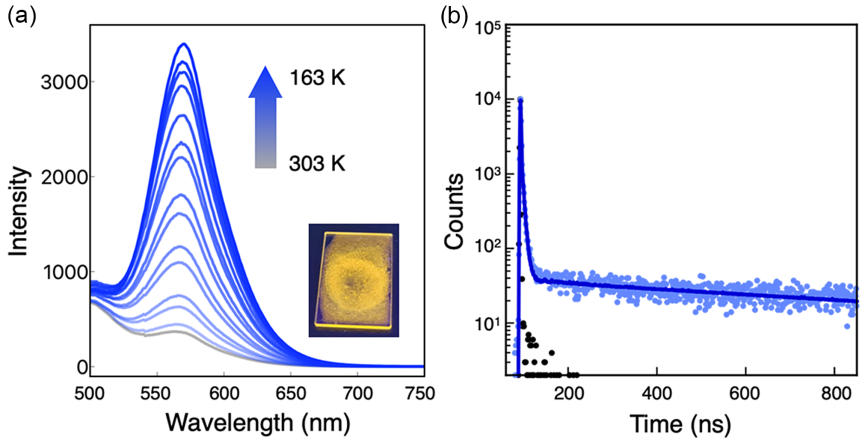


**Figure 5.** a) Variable-temperature photoluminescence spectra ($\lambda_{ex} = 470$ nm) of $Cl@Ag_{14}(\mathbf{1})_{12}$ in the solid state. Inset is a photograph of the film under irradiation from UV light (365 nm). b) Emission-lifetime decay profile of $Cl@Ag_{14}(\mathbf{1})_{12}$ in the solid state (light-blue dots) at 173 K ($\lambda_{ex} = 375$ nm). The instrumental response function (black dots) is also shown. The decay profile can be fitted using a multiexponential curve consisting of two components attributed to $Cl@Ag_{14}(\mathbf{1})_{12}$ and scattered light.

microsecond component suggests the involvement of the triplet excited state.[10c,31] However, details of this assignment are currently under further investigation.

Density functional theory calculations at the CAM-B3LYP/6-31G(d) (for H, C, N, Cl) and LANL2DZ (for Ag) level were conducted for monomeric $Cl@Ag_{14}(\mathbf{1})_{12}$ with or without six pyridyl groups coordinating to the corresponding silver centers, as a model for mutual coordination in the crystalline lattice (Figure S19, Supporting Information). To simulate the charge distribution on the cluster cores, we employed a natural population analysis (NPA), which is relatively realistic and basis-set independent compared to the Mulliken scheme.[33] Notably, NPA indicated a desymmetrized charge distribution on the $Ag_{14}$ core (**Figure 6**), and this tendency was enhanced for the pyridyl-coordinated model mentioned above, i.e., the Ag atoms coordinated by neighboring pyridyl groups are more positively charged than the other Ag atoms, while no significant bias was observed for the free monomer model (Figure S20 and S21, Supporting Information). These results conceptually indicate that the formation of 3D networking paves the way toward obtaining novel properties and functionalities in atomically precise metal NCs while maintaining their typical characters such as photoluminescence mentioned above.

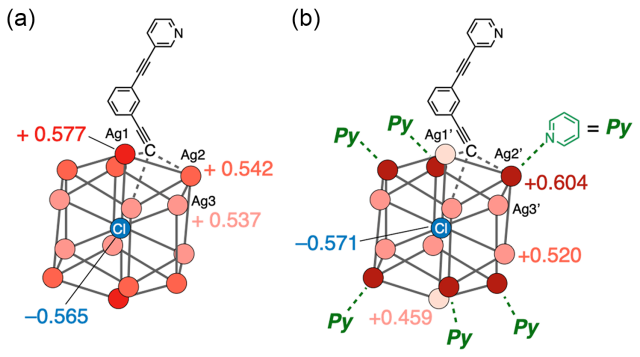


**Figure 6.** Schematic illustrations showing the natural charge distribution of a) $Cl@Ag_{14}(\mathbf{1})_{12}$ and b) $Cl@Ag_{14}(\mathbf{1})_{12}(pyridine)_6$. Ligands (except for representative depictions) are omitted for clarity, and the coordinating pyridine models are depicted as Py. The more positively charged silver atoms are shown in darker red.

## 3. Conclusion

In conclusion, we have successfully demonstrated the self-assembly of a silver NC based on the mutual coordination of acetylidic and pyridyl donors. The demonstrated strategy using a simple bifunctional ligand can be expected to facilitate the construction of NCs that are spatially aligned in a variety of 3D topologies by modifying the benzene ring motif in the ligand scaffold, which is currently in progress in our laboratory. In addition, the development of stimuli-responsive functions applicable to smart nanomaterials[34] can be expected, taking advantage of the dynamic properties provided by pyridyl coordination, which are potentially responsive to external environmental factors.[8]

## *Supporting Information*

The authors have cited additional references within the Supporting Information.[35–40]

## *Acknowledgements*

T.T. and T.N. contributed equally to this work. This research was supported by JSPS KAKENHI grants 22K05076 (to Y.D.), 19H05461 (to M.F.), and 24K01576 (to H.H.). Y.D. gratefully acknowledges financial support from the Toshiaki Ogasawara Memorial Foundation, the Shorai Foundation for Science and Technology, the Takahashi Industrial and Economic Research Foundation, the Noguchi Institute, and the Amano Institute of Technology. Synchrotron X-ray crystallography and X-ray absorption fine structure analysis were performed at the BL26B1, BL41XU, and BL36XU beamlines of SPring-8 under proposal numbers

Research Article
doi.org/10.1002/ceur.202500069



2023B2549, 2023A1118, 2023A1371, and 2024A1123. The authors are grateful to Dr. Kota Sakamoto for support with the XPS analysis. The NMR measurements were partly performed at the Center for Instrumental Analysis (Gunma University). The microscopic UV–vis analysis was performed at the Center for Analytical Instrumentation (Chiba University). A part of this work was supported by the Research Network and Facility Services Division in the National Institute for Materials Science (NIMS). The computations were performed using resources of the Research Center for Computational Science, Okazaki, Japan (under project numbers 22-IMS-C282, 23-IMS-C210, and 24-IMS-C236).

## Conflict of Interest

The authors declare no conflict of interest.

## Data Availability Statement

The data that support the findings of this study are available from the corresponding author upon reasonable request.

**Keywords:** acetylide · coordination polymers · self-assembly · silver nanoclusters · supramolecule

[1] a) R. Jin, C. Zeng, M. Zhou, Y. Chen, *Chem. Rev.* **2016**, *116*, 10346; b) I. Chakraborty, T. Pradeep, *Chem. Rev.* **2017**, *117*, 8208; c) Y. Li, R. Jin, *J. Am. Chem. Soc.* **2020**, *142*, 13627.

[2] a) J. Yang, R. Jin, *ACS Mater. Lett.* **2019**, *1*, 482; b) Y. Horita, M. Ishimi, Y. Negishi, *Sci. Technol. Adv. Mater.* **2023**, *24*, 2203832; c) Y. Sunada, K. Yamaguchi, K. Suzuki, *Coord. Chem. Rev.* **2022**, *469*, 214673.

[3] a) K. Konishi, M. Iwasaki, M. Sugiuchi, Y. Shichibu, *J. Phys. Chem. Lett.* **2016**, *7*, 4267; b) X. Kang, M. Zhu, *Chem. Soc. Rev.* **2019**, *48*, 242; c) J. Yan, B. K. Teo, N. Zheng, *Acc. Chem. Res.* **2018**, *51*, 3084; d) L. Shang, J. Xu, G. U. Nienhaus, *Nano Today* **2019**, *28*, 100767.

[4] a) E. Banach, T. Bürgi, *Helv. Chim. Acta* **2022**, *105*, e202100186; b) Y. Saito, C. Murata, M. Sugiuchi, Y. Shichibu, K. Konishi, *Coord. Chem. Rev.* **2022**, *470*, 214713.

[5] a) B. Yoon, W. D. Luedtke, R. N. Barnett, J. Gao, A. Desireddy, B. E. Conn, T. Bigioni, U. Landman, *Nat. Mater.* **2014**, *13*, 807; b) H. Li, P. Wang, C. Zhu, W. Zhang, M. Zhou, S. Zhang, C. Zhang, Y. Yun, X. Kang, Y. Pei, M. Zhu, *J. Am. Chem. Soc.* **2022**, *144*, 23205.

[6] J. V. Rival, P. Mymoona, K. M. Lakshmi, Nonappa, T. Pradeep, E. S. Shibu, *Small* **2021**, *17*, 2005718.

[7] a) S. Biswas, S. Das, Y. Negishi, *Coord. Chem. Rev.* **2023**, *492*, 215255; b) M. Bodiuzzaman, A. Nag, R. P. Narayanan, A. Chakraborty, R. Bag, G. Paramasivam, G. Natarajan, G. Sekar, S. Ghosh, T. Pradeep, *Chem. Commun.* **2019**, *55*, 5025; c) N. Kito, S. Takano, S. Masuda, K. Harano, T. Tsukuda, *Bull. Chem. Soc. Jpn.* **2023**, *96*, 1045; d) S. Zhang, Z. Zhang, R. Cao, *Inorg. Chim. Acta* **2017**, *461*, 57.

[8] a) R. S. Forgan, J.-P. Sauvage, J. F. Stoddart, *Chem. Rev.* **2011**, *111*, 5434; b) M. M. J. Smulders, I. A. Riddell, C. Brown, J. R. Nitschke, *Chem. Soc. Rev.* **2013**, *42*, 1728; c) T. R. Cook, J. P. Stang, *Chem. Rev.* **2015**, *115*, 7001; d) K. Harris, D. Fujita, M. Fujita, *Chem. Commun.* **2013**, *49*, 6703; e) S. D. P. Fielden, D. A. Leigh, S. L. Woltering, *Angew. Chem., Int. Ed.* **2017**, *56*, 11166.

[9] a) S.-F. Yuan, Z.-J. Guan, W.-D. Liu, Q.-M. Wang, *Nat. Commun.* **2019**, *10*, 4032; b) M.-M. Zhang, K.-K. Gao, X.-Y. Dong, Y. Si, T. Jia, Z. Han, S.-Q. Zang, T. C. W. Mak, *J. Am. Chem. Soc.* **2023**, *145*, 22310; c) A. Sarwa, A. Białońska, M. Garbicz, B. Szyszko, *Chem. Eur. J.* **2023**, *29*, e202203850; d) A. Sarwa, A. Khmara, K. A. Konieczny, D. Kulesza, E. Zych, B. Trzaskowski, B. Szyszko, *Angew. Chem., Int. Ed.* **2025**, e202423962.

[10] a) Z. Lei, X.-L. Pei, Z.-G. Jiang, Q.-M. Wang, *Angew. Chem., Int. Ed.* **2014**, *53*, 12771; b) M. J. Alhilaly, R.-W. Huang, R. Naphade, B. Alamer, M. N. Hedhili, A.-H. Emwas, P. Maity, J. Yin, A. Shkurenko, O. F. Mohammed, M. Eddaoudi, O. M. Bakr, *J. Am. Chem. Soc.* **2019**, *141*, 9585; c) R.-W. Huang, Y.-S. Wei, X.-Y. Dong, X.-H. Wu, C.-X. Du, S.-Q. Zang, T. C. W. Mak, *Nat. Chem.* **2017**, *9*, 689; d) X.-Y. Dong, H.-L. Huang, J.-Y. Wang, H.-Y. Li, S.-Q. Zang, *Chem. Mater.* **2018**, *30*, 2160; e) R.-W. Huang, X.-Y. Dong, B.-J. Yan, X.-S. Du, D.-H. Wei, S.-Q. Zang, T. C. W. Mak, *Angew. Chem., Int. Ed.* **2018**, *57*, 8560; f) W. A. Das, A. Jana, K. S. Sugi, G. Paramasivam, M. Bodiuzzaman, E. Khatun, A. Som, A. Mahendranath, A. Chakraborty, T. Pradeep, *Chem. Mater.* **2022**, *34*, 4703.

[11] a) A. N. Khlobystov, A. J. Blake, N. R. Champness, D. A. Lemenovskii, A. G. Majouga, N. V. Zyk, M. Schröder, *Coord. Chem. Rev.* **2001**, *222*, 155; b) P. J. Steel, C. M. Fitchett, *Coord. Chem. Rev.* **2008**, *252*, 990; c) T. Sawada, M. Fujita, *Chem* **2020**, *6*, 1861; d) J. Martí-Rujas, A. Famulari, *Angew. Chem., Int. Ed.* **2024**, *63*, e202407626.

[12] a) S. S. Y. Chui, M. F. Y. Ng, C.-M. Che, *Chem.-Eur. J.* **2005**, *11*, 1739; b) Q. Liang, X. Chang, Y.-Q. Su, S. M. Mugo, Q. Zhang, *Angew. Chem., Int. Ed.* **2021**, *60*, 18014.

[13] a) A. K. Gupta, A. Orthaber, *Chem.-Eur. J.* **2018**, *24*, 7536; b) Z. Lei, X.-K. Wan, S.-F. Yuan, Z.-J. Guan, Q.-M. Wang, *Acc. Chem. Res.* **2018**, *51*, 2465; c) M.-M. Zhang, X.-Y. Dong, Y.-J. Wang, S.-Q. Zang, T. C. W. Mak, *Coord. Chem. Rev.* **2022**, *453*, 214315.

[14] a) P. Maity, H. Tsunoyama, M. Yamauchi, M. Xie, S. Xie, T. Tsukuda, *J. Am. Chem. Soc.* **2011**, *133*, 20123; b) P. Maity, S. Takano, S. Yamazoe, T. Wakabayashi, T. Tsukuda, *J. Am. Chem. Soc.* **2013**, *135*, 9450; c) L. Qin, F. Sun, X. Ma, G. Ma, Y. Tang, L. Wang, Q. Tang, R. Jin, Z. Tang, *Angew. Chem., Int. Ed.* **2021**, *60*, 26136; d) F. Hu, R.-L. He, Z.-J. Guan, C.-Y. Liu, Q.-M. Wang, *Angew. Chem., Int. Ed.* **2023**, *62*, e202304134; e) J.-J. Li, Z. Liu, Z.-J. Guan, X.-S. Han, W.-Q. Shi, Q.-M. Wang, *J. Am. Chem. Soc.* **2022**, *144*, 690.

[15] a) H. Lang, A. Jakob, B. Milde, *Organometallics* **2012**, *31*, 7661; b) G. Fang, X. Bi, *Chem. Soc. Rev.* **2015**, *44*, 8124; c) P. E. Barran, H. L. Cole, S. M. Goldup, D. A. Leigh, P. R. McGonigal, M. D. Symes, J. Wu, M. Zengerle, *Angew. Chem., Int. Ed.* **2011**, *50*, 12280.

[16] a) G. S. Lewandos, D. K. Gregston, F. R. Nelson, *J. Organomet. Chem.* **1976**, *118*, 363; b) T. Nishinaga, T. Kawamura, K. Komatsu, *Chem. Commun.* **1998**, 2263.

[17] a) A. Martín-Lasanta, L. Á. de Cienfuegos, A. Johnson, D. Miguel, A. J. Mota, A. Orte, M. J. Ruedas-Rama, M. Ribagorda, D. J. Cárdenas, M. C. Carreño, A. M. Echavarren, J. M. Cuerva, *Chem. Sci.* **2014**, *5*, 4582; b) G.-T. Xu, X.-Y. Chang, K.-H. Low, L.-L. Wu, Q. Wan, H.-X. Shu, W.-P. To, J.-S. Huang, C.-M. Che, *Angew. Chem., Int. Ed.* **2022**, *61*, e202200748; c) S. Ibáñez, E. Peris, *Chem.-Eur. J.* **2018**, *24*, 8424.

[18] a) Y. Domoto, M. Abe, T. Kikuchi, M. Fujita, *Angew. Chem., Int. Ed.* **2020**, *59*, 3450; b) Y. Domoto, M. Abe, K. Yamamoto, T. Kikuchi, M. Fujita, *Chem. Sci.* **2020**, *11*, 10457; c) Y. Domoto, M. Abe, M. Fujita, *J. Am. Chem. Soc.* **2021**, *143*, 8578; d) Y. Domoto, K. Yamamoto, S. Horie, Z. Yu, M. Fujita, *Chem. Sci.* **2022**, *13*, 4372; e) Y. Domoto, M. Abe, G. R. Genov, Z. Yu, M. Fujita, *Angew. Chem., Int. Ed.* **2023**, *62*, e202303714; f) Y. Domoto, R. Nakabayashi, T. Tsurumi, H. Hayashi, Y. Nakamura, M. Fujita, *Chem.-Asian J.* **2025**, *20*, e202401378.

[19] a) Y. Domoto, M. Fujita, *Coord. Chem. Rev.* **2022**, *466*, 214605; b) Y. Domoto, *J. Incl. Phenom. Macrocycl. Chem.* **2025**, https://doi.org/10.1007/s10847-025-01297-x.

[20] Deposition numbers 2387233 (for $Cl@Ag_{14}(\mathbf{1})_{12}$ (OTf salt)) and 2418786 (for $Cl@Ag_{14}(\mathbf{1})_{12}$ ($SbF_6$ salt)) contain the supplementary crystallographic data for this paper. These data are provided free of charge by the joint Cambridge Crystallographic Data Centre and Fachinformationszentrum Karlsruhe Access Structures service.

[21] a) D. Rais, J. Yau, D. M. P. Mingos, R. Vilar, A. J. P. White, D. J. Williams, *Angew. Chem., Int. Ed.* **2001**, *40*, 3464; b) Z. Ren, J.-J. Sun, L. Xu, R. Luo, Z.-W. Ma, S. Li, Y.-B. Si, X.-Y. Dong, F. Pan, *Nanoscale* **2024**, *16*, 2662.

[22] S. C. K. Hau, P.-S. Cheng, T. C. W. Mal, *J. Am. Chem. Soc.* **2012**, *134*, 2922.

[23] Z.-R. Yuan, Z. Wang, B.-L. Han, C.-K. Zhang, S.-S. Zhang, Z.-Y. Zhu, J.-H. Yu, T.-D. Li, Y.-Z. Li, C.-H. Tung, D. Sun, *Angew. Chem., Int. Ed.* **2022**, *61*, e202211628.

[24] Feng Hu, J.-J. Li, Z.-J. Guan, S.-F. Yuan, Q.-M. Wang, *Angew. Chem., Int. Ed.* **2020**, *59*, 5312.

[25] K. Yonesato, H. Ito, D. Yokogawa, T. Kikuchi, N. Mizuno, K. Yamaguchi, K. Suzuki, *J. Am. Chem. Soc.* **2019**, *141*, 19550.

[26] a) G. Schön, *Acta Chem. Scand.* **1973**, *27*, 2623; b) A. M. Ferraria, A. P. Carapeto, A. M. Botelho do Rego, *Vacuum* **2012**, *86*, 1988.

[27] R. Frahm, *Nucl. Instrum. Methods Phys. Res., Sect. A* **1988**, *270*, 578.

[28] H. Ofuchi, T. Matsumoto, T. Honma, *Radiat. Phys. Chem.* **2024**, *218*, 111581.

Research Article
doi.org/10.1002/ceur.202500069

[29] In these measurements, excitation at 470 nm was used to minimize photo-irradiation damage to the cluster.
[30] The ligand **1•H** showed no absorption at 360–480 nm (Figure S16, Supporting Information).
[31] a) Y.-Z. Huang, R. K. Gupta, G.-G. Luo, Q.-C. Zhang, D. Sun, *Coord. Chem. Rev.* **2024**, *499*, 215508; b) S. Sharma, K. Kaushik, A. Salam, R. Garg, J. Mondal, R. Lamba, M. Kaur, C. K. Nandi, *ACS Appl. Nano Mater.* **2024**, *7*, 32; c) H. Fakhouri, M. P. Bakulić, I. Zhang, H. Yuan, D. Bain, F. Rondepierre, P.-F. Brevet, Ž. S. Maršić, R. Antoine, V. Bonačić-Koutecký, D. Maysinger, *Commun. Chem.* **2023**, *6*, 97.
[32] G.-X. Duan, L. Tian, J.-B. Wen, L.-Y. Li, Y.-P. Xie, X. Lu, *Nanoscale* **2018**, *10*, 18915.
[33] a) A. E. Reed, R. B. Weinstock, F. Weinhold, *J. Chem. Phys.* **1985**, *83*, 735; b) R. R. Zope, T. Baruah, *Phys. Rev. A* **2001**, *64*, 053202; c) K. Yonesato, S. Yamazoe, S. Kikkawa, D. Yokogawa, K. Yamaguchi, K. Suzuki, *Chem. Sci.* **2022**, *13*, 5557.
[34] S. Li, N.-N. Li, X.-Y. Dong, S.-Q. Zang, T. C. W. Mak, *Chem. Rev.* **2024**, *124*, 7262.

Manuscript received: March 24, 2025
Revised manuscript received: April 2, 2025
Version of record online: April 11, 2025